



## Discover Generics

Cost-Effective CT & MRI Contrast Agents

**FRESENIUS  
KABI**

[WATCH VIDEO](#)

# AJNR

This information is current as  
of June 24, 2025.

## **Comparison of Enhancement of the Vestibular Perilymph between Variable and Constant Flip Angle–Delayed 3D-FLAIR Sequences in Menière Disease**









S. Nahmani, A. Vaussy, C. Hautefort, J.-P. Guichard, A.  
Guillonet, E. Houdart, A. Attyé and M. Eliezer

*AJNR Am J Neuroradiol* 2020, 41 (4) 706-711

doi: <https://doi.org/10.3174/ajnr.A6483>

<http://www.ajnr.org/content/41/4/706>

# Comparison of Enhancement of the Vestibular Perilymph between Variable and Constant Flip Angle–Delayed 3D-FLAIR Sequences in Menière Disease

 S. Nahmani,  A. Vaussy,  C. Hautefort,  J.-P. Guichard,  A. Guillonet,  E. Houdart,  A. Attyé, and  M. Eliezer



## ABSTRACT

**BACKGROUND AND PURPOSE:** Endolymphatic hydrops in patients with Menière disease relies on delayed postcontrast 3D-FLAIR sequences. The purpose of this study was to compare the degree of perilymphatic enhancement and the detection rate of endolymphatic hydrops using constant and variable flip angles sequences.

**MATERIALS AND METHODS:** This was a retrospective study performed in 16 patients with Menière disease who underwent 3T MR imaging 4 hours after gadolinium injection using two 3D-FLAIR sequences with a constant flip angle at 140° for the first and a heavily-T2 variable flip angle for the second. The signal intensity ratio was measured using the ROI method. We graded endolymphatic hydrops and evaluated the cochlear blood-labyrinth barrier impairment.

**RESULTS:** Both for symptomatic and asymptomatic ears, the median signal intensity ratio was significantly higher with the constant flip angle than with the heavily-T2 variable flip angle (7.16 versus 1.54 and 7.00 versus 1.45,  $P < .001$ ). Cochlear blood-labyrinth barrier impairment was observed in 4/18 symptomatic ears with the heavily-T2 variable flip angle versus 8/19 with constant flip angle sequences. With heavily-T2 variable flip angle sequences, endolymphatic hydrops was observed in 7–10/19 symptomatic ears versus 12/19 ears with constant flip angle sequences. We found a significant association between the clinical symptomatology and the presence of endolymphatic hydrops with constant flip angle but not with heavily-T2 variable flip angle sequences. Interreader agreement was always perfect with constant flip angle sequences while it was fair-to-moderate with heavily-T2 variable flip angle sequences.

**CONCLUSIONS:** 3D-FLAIR constant flip angle sequences provide a higher signal intensity ratio and are superior to heavily-T2 variable flip angle sequences in reliably evaluating the cochlear blood-labyrinth barrier impairment and the endolymphatic space.

**ABBREVIATIONS:** BLB = blood-labyrinth barrier; CFA = constant flip angle; EH = endolymphatic hydrops; hVFA = heavily-T2 variable flip angle; MD = Menière disease; SIR = signal intensity ratio; VFA = variable flip angle

Menière Disease (MD), consisting of recurrent spells of spontaneous vertigo and fluctuating aural symptoms, is associated with endolymphatic hydrops (EH), which is an accumulation of excessive endolymph fluid in the inner ear, but also with blood-labyrinth barrier (BLB) impairment.<sup>1–3</sup>

During the past decade, to define EH on MR imaging, most studies have used the semiquantitative grading system introduced


by the nakashima et al., while some authors have suggested that this grading system was not specific.<sup>2</sup> On the basis of these findings, an anatomic grading system based on the saccular morphology in combination with cochlear BLB impairment has been introduced.<sup>4,5</sup>

There are 2 reported methods for contrast media administration: intratympanic and intravenous.<sup>6,7</sup> The main advantage of an intratympanic administration is a higher perilymphatic contrast, allowing the use of 3D-real inversion recovery sequences, which are less sensitive to gadolinium but enable the visualization of endolymph, perilymph, and bone in a single image.<sup>8,9</sup> However, due to its invasiveness, the intratympanic method has been replaced by the intravenous method.<sup>9</sup> It requires a shorter waiting time (4 hours) and allows the evaluation of the permeability of the BLB in both ears. 3D-FLAIR sequences, which are more sensitive to T1-shortening than 3D-real inversion recovery sequences, were adjusted to enable the best evaluation of EH.<sup>10</sup>

Received July 26, 2019; accepted after revision February 12, 2020.

From the Departments of Neuroradiology (S.N., J.-P.G., A.G., E.H., M.E.), and Head and Neck Surgery (C.H.), Lariboisière University Hospital, Paris, France; Siemens Healthineers (A.V.), Saint-Denis, France; and Department of Neuroradiology and MRI (A.A.), Grenoble Alpes University Hospital, SFR RMN Neurosciences, Grenoble, France.

Please address correspondence to Michael Eliezer, MD, Neuroradiology Unit, Lariboisière University Hospital, 75010 Paris, France; e-mail: michael.eliezer@aphp.fr

 Indicates article with supplemental on-line table.

<http://dx.doi.org/10.3174/ajnr.A6483>

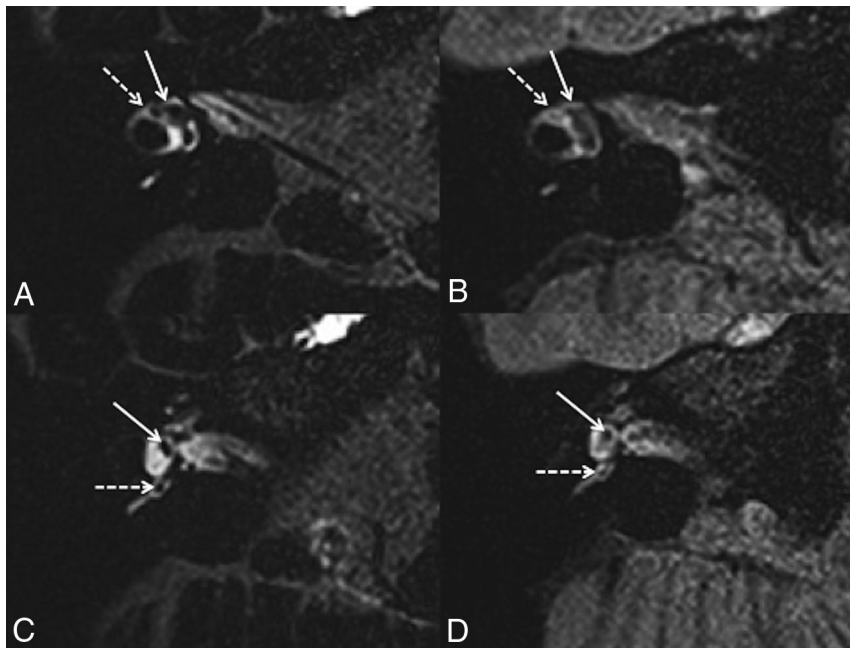


**FIG 1.** A 42-year-old woman with right possible MD. Axial 3D-FLAIR CFA at the level of the lateral semicircular canal (A) shows a normal utricle (white arrow) and lateral ampulla (right dotted arrow). C, Axial 3D-FLAIR CFA through the inferior part of the vestibule shows a normal saccule (white arrow) and posterior ampulla (white dotted arrow). Axial 3D-FLAIR heavily-T2 VFA at the level of the lateral semicircular canal (B) shows a normal utricle (white arrow), while the lateral ampulla (right dotted arrow) is barely visible. D, Axial 3D-FLAIR heavily-T2 VFA through the inferior part of the vestibule shows a normal saccule (white arrow) and posterior ampulla (white dotted arrow).

In the same way, a postprocessing technique implying a fusion of gray-scale inverted positive endolymph with native positive perilymph images has been developed to overcome the lower contrast obtained after intravenous injection.<sup>11</sup> Other authors reported that 3D-FLAIR sequences using a constant flip angle (CFA) instead of a variable flip angle (VFA), without postprocessing, were self-sufficient to provide a good contrast-to-noise ratio.<sup>12-14</sup> However, to this day, VFA sequences remain more widespread than CFA sequences because of their lower specific absorption rate deposition and enable reducing scan times by increasing the echo-train length without blurring.<sup>15</sup>

In a previous study, Naganawa et al<sup>16</sup> stated that the 3D-FLAIR heavily-T2 variable flip angle (hVFA) was superior to CFA sequences in improving the contrast-to-noise ratio and the recognition of the endolymphatic space compartments. Yet, different acquisition parameters between both sequences were used; thus, no proper comparison should be made.

The purpose of this study was to compare the degree of perilymphatic enhancement and the detection rate of EH in patients with MD using CFA and hVFA sequences with equivalent technical parameters.

## MATERIALS AND METHODS

### Patients

This was a retrospective imaging study approved by our institutional review board (Lariboisiere University Hospital; IRB 2214440) and conducted between December 2018 and March

2019. Patients with a clinical diagnosis of definite, probable, and possible MD based on the 1995 American Academy of Otolaryngology-Head and Neck Surgery recommendations were included.<sup>17</sup> Patients with a history of intratympanic treatment or operations were excluded.

### Audiometric Test

The mean pure-tone average hearing levels measured at 500, 1000, 2000, and 4000 Hz in each ear were evaluated. When symptoms were bilateral, we considered both ears as symptomatic.

### Imaging

MR imaging examinations were performed on a 3T Magnetom Skyra scanner (Siemens, Erlangen, Germany) with a head/neck 64 coil. All patients underwent MR imaging 4 hours after a single intravenous dose of gadobutrol (Gadovist, 0.1 mmol/kg, 1 mmol/mL; Bayer Schering Pharma, Berlin, Germany), which provided high contrast in the labyrinth.<sup>18</sup> We performed two 3D-FLAIR MR imaging sequences. The first was acquired with a CFA (140°) and the second with a VFA.

We performed the 3D-FLAIR sequences with the following parameters: FOV = 140 × 140 mm, TR = 10,000 ms, TE = 640 ms, TI = 2600 ms, matrix size = 256 × 256 mm, NEX = 2, generalized autocalibrating partially parallel acquisition = 2, section thickness = 0.8 mm, scan time = 7 minutes 50 seconds.

### Imaging Analysis

For each patient, MR images were evaluated independently with Carestream Vue (Carestream health) 12.1 by 2 readers (A = S.N. and B = M.E.) with, respectively, 1 and 6 years of experience in inner ear imaging, blinded to the clinical data.

**Quantitative Assessment.** Quantitative assessment of the BLB permeability was performed with the ROI method, as previously reported.<sup>14</sup> A 5-mm<sup>2</sup> circular ROI was placed in the basal turn of the cochlea and a 50-mm<sup>2</sup> circular ROI was placed at the same level in the medulla. The signal intensity ratio (SIR) was defined as the signal intensity of the basal turn divided by that of the medulla. The mean SIR value was calculated for each ear.

**Qualitative Assessment.** We verified the presence of the following structures (Fig 1): 1) the saccule, an area of hypointense signal located at the medial and anterior walls of the vestibule at the level of the oval window;<sup>19,20</sup> 2) the utricle, an elliptic area of hypointense signal located in the superior part of the vestibule at the level of the lateral semicircular canal;<sup>19,20</sup> and 3) the ampulla of each semicircular canal, an area of hypointense signal surrounded by perilymphatic fluid.

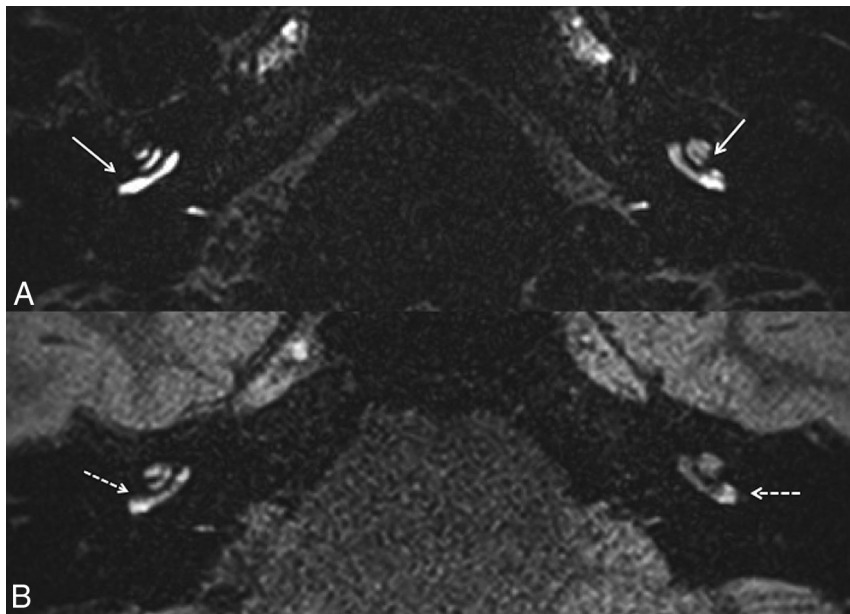


**FIG 2.** A 63-year-old woman with right definite MD. A, Axial CFA at the level of the basal turn of the cochlea shows a marked right cochlear BLB impairment compared with the left side (white arrow). B, The right cochlear BLB impairment (white dotted arrow) is less obvious with hVFA.

We used a modified EH grading system according to Bernaerts et al<sup>5</sup> and defined the presence of EH when the saccule became equal to or larger than the utricle or when there was a confluence of the saccule and utricle.<sup>4</sup> We also assessed the presence of cochlear BLB impairment, defined as a subjective marked perilymphatic enhancement in the basal turn of the cochlea (0, no BLB impairment; 1, BLB impairment) relative to the contralateral cochlea, as previously reported.<sup>5</sup>

A visual assessment based on a binary scale was performed to evaluate the distinction between the utricle and the saccule, and the ampullas from the perilymphatic space (0, no distinction; 1, distinction).

### Statistical Analysis

Data were analyzed using R statistical and computing software, Version 3.3.2 (<http://www.r-project.org/>). Comparison of SIR between CFA and hVFA sequences was assessed with the Wilcoxon signed ranked test. Comparison of the SIR between symptomatic and asymptomatic ears was assessed by the Mann-Whitney test. Comparison for visual assessment between CFA and hVFA sequences was made using the Fisher exact test. Interreader agreement was calculated with the Cohen  $\kappa$  coefficient, to evaluate the reproducibility of the qualitative analysis. Continuous data were expressed as medians (Q1; Q3) and ranges. Categorical data were expressed as frequencies and percentages. Significance was set at  $P < .05$ .

## RESULTS

### Population

Sixteen patients with MD (10 women and 6 men, 7 with right-sided MD, 6 with left-sided MD, and 3 with bilateral MD) with a median age of 46 years (Q1: 43 years, Q3: 52 years; range, 35–68

years) were included in this study. A total of 32 ears were analyzed, including 19 symptomatic and 13 asymptomatic ears.

The median of the pure-tone average levels in the symptomatic ears was 23 dB (Q1: 17 dB, Q3: 50 dB; range, 4–73 dB), and 15 dB (Q1: 15 dB, Q3: 19 dB; range, 3–34 dB) in the asymptomatic ears.

### MR Imaging Data

**Quantitative Analysis.** For the symptomatic ears, the SIR was significantly lower with hVFA (median, 1.54; Q1: 1.44, Q3: 1.84; range, 0.93–2.55) than with CFA (median, 7.16; Q1: 5.65, Q3: 8.46; range, 4.39–15.71) ( $P < .001$ ).

For the asymptomatic ears, there were also significant differences in the SIR between hVFA (median, 1.45; Q1: 1.30, Q3: 1.68; range, 1.10–1.91) and CFA sequences (median, 7; Q1: 5.85, Q3: 7.6; range, 4.65–11.04) ( $P < .001$ ).

No significant differences in the SIR were found between symptomatic and asymptomatic ears, either with CFA ( $P = .70$ ) or hVFA sequences ( $P = .25$ ).

**Qualitative Analysis. Cochlear Blood Labyrinth Barrier Impairment.** With hVFA sequences (Fig 2), cochlear BLB impairment was observed in 6/32 ears (18.7%) (6/19 symptomatic and 0/13 asymptomatic ears) according to reader A and 4/32 ears (12.5%) according to reader B (4/19 symptomatic, 0/13 asymptomatic ears). The Cohen  $\kappa$  coefficient was 0.53. There was no significant association between cochlear BLB impairment and clinical symptomatology ( $P = .06$  for reader A and  $P = .12$  for reader B).

With CFA sequences (Fig 2), cochlear BLB impairment was observed in 8/32 ears (25.0%) according to both readers (8/19 symptomatic and 0/13 asymptomatic ears). Interreader agreement was perfect (Cohen  $\kappa$  coefficient = 1). There was a significant association between cochlear BLB impairment and clinical symptomatology ( $P = .01$ ).

Data are summarized in the On-line Table.

**Endolymphatic Hydrops.** With hVFA sequences (Fig 3), EH was observed in 13/32 ears (40.6%) according to reader A (10/19 symptomatic and 3/13 asymptomatic ears) and 10/32 ears (31.3%) according to reader B (7/19 symptomatic and 3/13 asymptomatic ears). The Cohen  $\kappa$  coefficient was 0.26. There was no significant association between the clinical symptomatology and the presence of EH ( $P = .15$ , OR = 3.55; 95% CI, 0.63–26.62; and  $P = .47$ , OR = 1.90; 95% CI, 0.32–14.47, according to readers A and B respectively).

With CFA sequences (Fig 3), both readers reported EH in 14/32 ears (43.7%: 12/19 symptomatic and 2/13 asymptomatic ears). The Cohen  $\kappa$  coefficient was 1. We found a significant association between the clinical symptomatology and the presence of EH ( $P = .01$ , OR = 8.73; 95% CI, 1.33 – 103.73).

Data are summarized in the On-line Table.



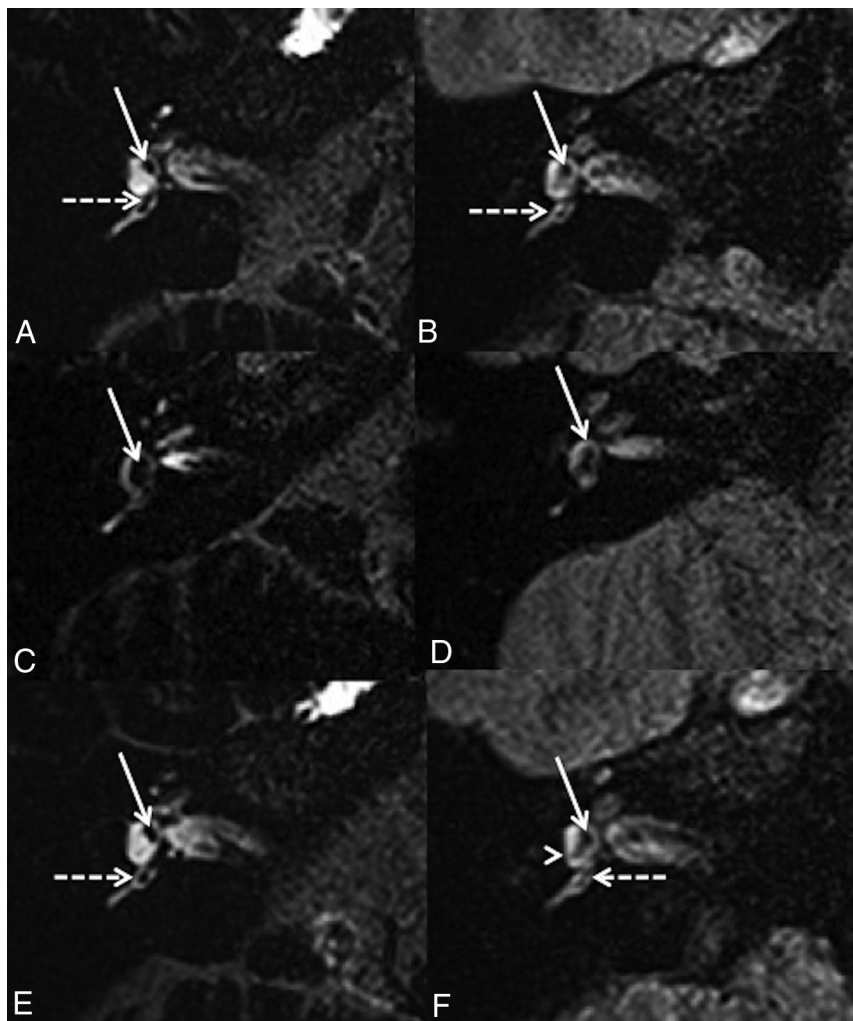


**FIG 3.** A 42-year-old woman with right possible MD. Right axial CFA (A) and hVFA (B) sequences through the inferior part of the vestibule show a normal saccule (white arrow) and posterior ampulla (white dotted arrow) in both sequences. A 43-year-old man with a right definite MD. Right axial CFA (C) and hVFA (D) sequences through the inferior part of the vestibule show saccular hydrops (white arrow) in both sequences. A 35-year-old woman with a right possible MD. Right axial CFA (E) and hVFA (F) sequences through the inferior part of the vestibule and the posterior ampulla (white dotted arrow). With the CFA sequence, the right saccule appears normal (white arrow). With the hVFA sequence, reader A described a right saccular hydrops, while reader B defined the right saccule as normal. The saccule (white arrow) and the posterior and lower parts of the utricle (white arrowhead) were confluent without expansion of these 2 structures.

**Endolymphatic Space Evaluation.** With hVFA sequences (Fig 3), the distinction between the utricle and the saccule was not possible in 13/32 ears (40.6%) according to reader A (8/19 symptomatic and 5/13 asymptomatic ears) and 13/32 ears (40.6%) according to reader B (9/19 symptomatic and 4/13 asymptomatic ears). The Cohen  $\kappa$  coefficient was 0.35. For both readers, there were no significant differences in the distinction between the utricle and the saccule whether the patient was symptomatic or not ( $P=1$  for reader A and  $P=.47$  for reader B). Among the ears in which the distinction between the saccule and the utricle was not possible, EH was described in only 6/13 ears (46.2%) according to reader A and 9/13 ears (69.2%) according to reader B.

The distinction of the posterior ampulla was not possible in 12/32 ears (37.5%) according to reader A (8/19 symptomatic and

4/13 asymptomatic ears) and 10/32 ears (31.3%) according to reader B (8/19 symptomatic and 2/13 asymptomatic ears). The Cohen  $\kappa$  coefficient was 0.31. The distinction of the lateral ampulla was not possible in 17/32 ears (53.1%) according to reader A (10/19 symptomatic and 7/13 asymptomatic ears) and 21/32 (65.6%) according to reader B (12/19 symptomatic and 9/13 asymptomatic ears). The Cohen  $\kappa$  coefficient was 0.49. For both readers, the absence of discrimination of the ampullas was not significantly related to the clinically symptomatic ear or the presence of endolymphatic hydrops.

With CFA sequences (Fig 3), the distinction between the utricle and the saccule was not possible in 10/32 ears (31.3%) for both readers (9/19 symptomatic and 1/13 asymptomatic ears). The Cohen  $\kappa$  coefficient was 1. Among the 10 ears in which the distinction between the utricle and the saccule was not possible, EH was identified in all ears according to both readers. There was a significant association between the absence of utricle/saccule discrimination and the clinically symptomatic ear (OR = 0.09; 95% CI, 0.01–0.93;  $P=.02$ ).

The distinction of the lateral and posterior ampullas was always observed for both readers. Interreader agreement was perfect (Cohen  $\kappa$  coefficient = 1).

Data are summarized in the Online Table.

## DISCUSSION

We demonstrated that CFA was superior to hVFA sequences for evaluating

the SIR, cochlear BLB impairment, and the endolymphatic space, with high reliability.

MR imaging evaluation of the endolymphatic space is based on the difference in signal between the endolymphatic and perilymphatic spaces due to the selective enhancement of the perilymphatic space after contrast media administration. In our study, SIR, which is an indirect evaluation of the contrast-to-noise ratio, was significantly higher with CFA than hVFA sequences. Naganawa et al<sup>11</sup> have reported the opposite association, yet the parameters of these 2 sequences were not strictly similar; thus, no proper comparison should be made.

In the literature, hVFA sequences are most commonly used for the diagnosis of EH because they allow keeping the high signal amplitude through the long readout duration.<sup>15</sup> After a 90°

radiofrequency pulse, equally spaced 180° radiofrequency pulses are the most appropriate ones to refocus transverse magnetization generating a train of spin echoes without compromising longitudinal relaxation. However, constant high flip angle refocusing radiofrequency pulses are responsible for high-power deposition in tissues, which must be monitored in the brain due to the specific absorption rate regulatory limits (2 W/kg).<sup>15</sup> VFA radiofrequency pulses have been designed to provide higher signal amplitude and low specific absorption rate deposition, by maintaining a transverse magnetization as well as using longitudinal magnetization to contribute to the signal during sequence readouts. It is based on the principle of stimulated echo, which cannot be reached by a 180° CFA. One of the consequences is a decrease in contrast in T1 due to a permanent residual transverse magnetization but also lower flip angle values. This is an obvious impediment in the EH imaging, in which the main focus is to highlight the shortening of the longitudinal relaxation induced by gadolinium. Thus, a constant 140° radiofrequency pulse has been found to be the best compromise to limit stimulated echoes, as well as specific absorption rate deposition. In our study, specific absorption rate deposition was around 0.03–0.05 W/kg with hVFA and 0.16–0.22 W/kg with CFA sequences.

We found a strong correlation between the cochlear BLB impairment and the symptomatic ear with CFA ( $P = .01$ ) but not with hVFA sequences ( $P = .06$  for reader A and  $P = .13$  for reader B). Hydrops protocol enables the assessment of not only the endolymphatic space but also the permeability of the BLB, which might be slightly impaired in MD but also in various inner ear diseases.<sup>13,14,21–24</sup> Various authors have demonstrated that some patients with MD could also have cochlear BLB impairment, either isolated or in association with EH.<sup>5,25</sup> Therefore, we recommend the use of CFA instead of hVFA sequences to evaluate the permeability of the BLB with a high reliability.

The distinction between the utricle and the saccule is crucial because the diagnosis of EH on MR imaging relies on the presence of saccular dilation.<sup>4</sup> However, in cases of severe dilation, one can observe an expansion of the dilation from the saccule to the utricle, making it impossible to distinguish these 2 structures. With CFA sequences, this distinction was not possible in 10 ears because EH was identified in all of them according to both readers. By contrast, with hVFA sequences, the utricle and the saccule could not be distinguished in 7 and 4 ears (respectively, for readers A and B), while no sign of EH was observed. Indeed, we observed cases in which the saccule and the utricle were not dilated but seemed to be confluent at a focal point with surrounding perilymphatic space.

EH in the asymptomatic ears was observed in 3 patients with MD with hVFA and CFA sequences. However, with hVFA sequences, both readers were in agreement on only 1 of these 3 patients. In the literature, the rate of EH in asymptomatic ears on MR imaging ranges from 20% to 65%.<sup>26,27</sup> Here, we propose the hypothesis that previously published discrepancies may be related to the use of different flip angle parameters in addition to the disease itself.

The distinction of the ampullas from the surrounding perilymphatic space is a strong indicator of the spatial resolution of

the sequence, which is highly recommended for hydrops protocol. Although ampullar hydrops is uncommon, lately, it has been reported that some patients with atypical acute vestibular syndrome could present with a collapse of the endolymphatic space of the pars superior (utricle and ampullas).<sup>28</sup> With CFA sequences, the visualization of the ampullas was possible in all cases, while this evaluation was more inconsistent with hVFA sequences.

### Therapeutic Applications

The treatment of MD is based on lifestyle change and various drug therapies for the management of vertigo.<sup>29</sup> More invasive treatments such as endolymphatic sac surgery, vestibular nerve section, or intratympanic drugs can be suggested in cases of medical treatment failure.<sup>30–32</sup> The pathophysiologic effect of endolymphatic sac surgery is still widely discussed and could be further discussed in light of results from the MR imaging hydrops protocol, suggesting that vestibular neurectomy should be preferred to control vertigo in patients without saccular hydrops.

Our study has several limitations, first, by its retrospective nature. Second, because 15% of patients with MD might present with EH on the contralateral asymptomatic ear, the presence of a control group would have been interesting. We had no possibility of quantifying the volume of the vestibular endolymphatic space in vivo; thus, it was not possible to assess whether the observed radiologic hydrops is well-correlated with the true presence of an endolymphatic hydrops in histopathology. Another limitation of our study was the small number of patients, which could explain some nonsignificant results. However, those results were only related to the hVFA sequences but never to the CFA sequences.

### CONCLUSIONS

The diagnosis of EH in patients with MD can be difficult on MR imaging because it requires fine analysis of small anatomic structures. When performing hydrops protocol, radiologists should keep in mind that FLAIR sequences require optimal parameters to evaluate the endolymphatic space and the permeability of the BLB accurately. We demonstrated that CFA sequences provided higher SIR and were superior to hVFA sequences in reliably evaluating the cochlear BLB impairment and the endolymphatic space.

### ACKNOWLEDGMENTS

We thank Pamela Haylock (Lariboisiere University Hospital) for critically editing the manuscript.

Disclosures: Alexis Vaussy—UNRELATED: Employment: Siemens Healthineers France, Comments: current MR Clinical Scientist position within the company. Arnaud Attyé—UNRELATED: Consultancy: Pixyl Medical, Comments: I have a consulting service agreement with occasional consultant activities; OTHER RELATIONSHIPS: I have conducted previous MRI studies on healthy volunteers' inner ears using research funds from Guerbet SA.

### REFERENCES

1. Altmann F, Fowler EP Jr. **Histological findings in Meniere's symptom complex.** *Ann Otol Rhinol Laryngol* 1943;52:52–80

2. Nakashima T, Naganawa S, Pyykko I, et al. Grading of endolymphatic hydrops using magnetic resonance imaging. *Acta Otolaryngol Suppl* 2009;5–8 [CrossRef Medline](#)
3. Tagaya M, Yamazaki M, Teranishi M, et al. Endolymphatic hydrops and blood-labyrinth barrier in Ménière's disease. *Acta Otolaryngol* 2011;131:474–79 [CrossRef Medline](#)
4. Attyé A, Eliezer M, Boudiaf N, et al. MRI of endolymphatic hydrops in patients with Meniere's disease: a case-controlled study with a simplified classification based on saccular morphology. *Eur Radiology* 2017;27:3138–46 [CrossRef Medline](#)
5. Bernaerts A, Vanspauwen R, Blaivie C, et al. The value of four stage vestibular hydrops grading and asymmetric perilymphatic enhancement in the diagnosis of Ménière's disease on MRI. *Neuroradiology* 2019;61:421–29 [CrossRef Medline](#)
6. Naganawa S, Komada T, Fukatsu H, et al. Observation of contrast enhancement in the cochlear fluid space of healthy subjects using a 3D-FLAIR sequence at 3 Tesla. *Eur Radiol* 2006;16:733–37 [CrossRef Medline](#)
7. Naganawa S, Yamazaki M, Kawai H, et al. Visualization of endolymphatic hydrops in Ménière's disease with single-dose intravenous gadolinium-based contrast media using heavily T(2)-weighted 3D-FLAIR. *Magn Reson Med Sci* 2010;9:237–42 [CrossRef Medline](#)
8. Yamazaki M, Naganawa S, Tagaya M, et al. Comparison of contrast effect on the cochlear perilymph after intratympanic and intravenous gadolinium injection. *AJNR Am J Neuroradiol* 2012;33:773–78 [CrossRef Medline](#)
9. Li Y, Sha Y, Wang F, et al. Comprehensive comparison of MR image quality between intratympanic and intravenous gadolinium injection using 3D real IR sequences. *Acta Otolaryngol* 2019;139:659–64 [CrossRef Medline](#)
10. Naganawa S. The technical and clinical features of 3D-FLAIR in neuroimaging. *Magn Reson Med Sci* 2015;14:93–106 [CrossRef Medline](#)
11. Naganawa S, Yamazaki M, Kawai H, et al. Imaging of Ménière's disease after intravenous administration of single-dose gadodiamide: utility of subtraction images with different inversion time. *Magn Reson Med Sci* 2012;11:213–19 [CrossRef Medline](#)
12. Sepahdari AR, Ishiyama G, Vorasubin N, et al. Delayed intravenous contrast-enhanced 3D FLAIR MRI in Meniere's disease: correlation of quantitative measures of endolymphatic hydrops with hearing. *Clin Imaging* 2015;39:26–31 [CrossRef Medline](#)
13. Eliezer M, Maquet C, Horion J, et al. Detection of intralabyrinthine abnormalities using post-contrast delayed 3D-FLAIR MRI sequences in patients with acute vestibular syndrome. *Eur Radiol* 2019;29:2760–69 [CrossRef Medline](#)
14. Pakdaman MN, Ishiyama G, Ishiyama A, et al. Blood-labyrinth barrier permeability in Meniere disease and idiopathic sudden sensorineural hearing loss: findings on delayed postcontrast 3D-FLAIR MRI. *AJNR Am J Neuroradiol* 2016;37:1903–08 [CrossRef Medline](#)
15. Mugler JP. Optimized three-dimensional fast-spin-echo MRI. *J Magn Reson Imaging* 2014;39:745–67 [CrossRef Medline](#)
16. Naganawa S, Kawai H, Sone M, et al. Increased sensitivity to low concentration gadolinium contrast by optimized heavily T2-weighted 3D-FLAIR to visualize endolymphatic space. *Magn Reson Med Sci* 2010;9:73–80 [CrossRef Medline](#)
17. Committee on Hearing and Equilibrium guidelines for the evaluation of results of treatment of conductive hearing loss: American Academy of Otolaryngology-Head and Neck Surgery Foundation, Inc. *Otolaryngol Head Neck Surg* 1995;113:186–87 [CrossRef Medline](#)
18. Eliezer M, Poillon G, Gillibert A, et al. Comparison of enhancement of the vestibular perilymph between gadoterate meglumine and gadobutrol at 3-Tesla in Meniere's disease. *Diagn Interv Imaging* 2018;99:271–77 [CrossRef Medline](#)
19. Merchant SN, Nadol JB. *Schuknecht's Pathology of the Ear*. 3rd ed. Shelton: McGraw-Hill Medical; 2010
20. Lane JI, Witte RJ, Bolster B, et al. State of the art: 3T imaging of the membranous labyrinth. *AJNR Am J Neuroradiol* 2008;29:1436–40 [CrossRef Medline](#)
21. Naganawa S, Kawai H, Taoka T, et al. Cochlear lymph fluid signal increase in patients with otosclerosis after intravenous administration of gadodiamide. *Magn Reson Med Sci* 2016;15:308–15 [CrossRef Medline](#)
22. Byun H, Chung JH, Lee SH, et al. The clinical value of 4-hour delayed-enhanced 3D-FLAIR MR images in sudden hearing loss. *Clin Otolaryngol* 2019;44:336–42 [CrossRef Medline](#)
23. Eliezer M, Toupet M, Guichard J-P, et al. Cochleovestibular artery syndrome: consideration based on VHIT, VEMP, and inner ear MRI. *J Neurol* 2019;266:2327–29 [CrossRef Medline](#)
24. Eliezer M, Verillaud B, Guichard J-P, et al. Labyrinthine infarction caused by vertebral artery dissection: consideration based on MRI. *J Neurol* 2019;266:2575–77 [CrossRef Medline](#)
25. Kahn L, Hautefort C, Guichard JP, et al. Relationship between video head impulse test, ocular and cervical vestibular evoked myogenic potentials and compartmental magnetic resonance imaging classification in Ménière's disease. *Laryngoscope* 2019 Nov 19. [Epub ahead of print] [CrossRef Medline](#)
26. Barath K, Schuknecht B, Naldi AM, et al. Detection and grading of endolymphatic hydrops in Meniere disease using MR imaging. *AJNR Am J Neuroradiol* 2014;35:1387–92 [CrossRef Medline](#)
27. Pyykkö I, Nakashima T, Yoshida T, et al. Meniere's disease: a reappraisal supported by a variable latency of symptoms and the MRI visualisation of endolymphatic hydrops. *BMJ Open* 2013;3:e001555 [CrossRef](#)
28. Eliezer M, Attyé A, Guichard JP, et al. Vestibular atelectasis: myth or reality?. *Laryngoscope* 2019;129:1689–95 [CrossRef Medline](#)
29. Sajjadi H, Paparella MM. Meniere's disease. *Lancet* 2008;372:406–14 [CrossRef Medline](#)
30. Sood AJ, Lambert PR, Nguyen SA, et al. Endolymphatic sac surgery for Ménière's disease: a systematic review and meta-analysis. *Otol Neurotol* 2014;35:1033–45 [CrossRef Medline](#)
31. Tewary AK, Riley N, Kerr AG. Long-term results of vestibular nerve section. *J Laryngol Otol* 1998;112:1150–53 [CrossRef Medline](#)
32. Miller MW, Agrawal Y. Intratympanic therapies for Meniere's disease. *Curr Otorhinolaryngol Rep* 2014;2:137–43 [CrossRef Medline](#)